

An Analytic Throughput Model for TCP NewReno

Nadim Parvez, Anirban Mahanti, and Carey Williamson, *Member, IEEE*

Abstract—This paper develops a simple and accurate stochastic model for the steady-state throughput of a TCP NewReno bulk data transfer as a function of round-trip time and loss behaviour. Our model builds upon extensive prior work on TCP Reno throughput models but differs from these prior works in three key aspects. First, our model introduces an analytical characterization of the TCP NewReno fast recovery algorithm. Second, our model incorporates an accurate formulation of NewReno’s timeout behaviour. Third, our model is formulated using a flexible two-parameter loss model that can better represent the diverse packet loss scenarios encountered by TCP on the Internet.

We validated our model by conducting a large number of simulations using the *ns-2* simulator and by conducting emulation and Internet experiments using a NewReno implementation in the BSD TCP/IP protocol stack. The main findings from the experiments are: (1) the proposed model accurately predicts the steady-state throughput for TCP NewReno bulk data transfers under a wide range of network conditions; (2) TCP NewReno significantly outperforms TCP Reno in many of the scenarios considered; and (3) using existing TCP Reno models to estimate TCP NewReno throughput may introduce significant errors.

Index Terms—TCP, analytical modeling, simulation, *ns-2*

I. INTRODUCTION

The Transmission Control Protocol (TCP) [33] provides reliable, connection-oriented, full-duplex, unicast data delivery on the Internet. Modern TCP implementations also include congestion control mechanisms that adapt the source transmission behaviour to network conditions by dynamically computing the *congestion window* size. The goal of TCP congestion control is to increase the congestion window size if there is additional bandwidth available on the network, and decrease the congestion window size when there is congestion. It is widely agreed that the congestion control schemes in TCP provide stability for the “best effort” Internet. These mechanisms increase network utilization, prevent starvation of flows, and ensure inter-protocol fairness [10].

In today’s Internet, several variants of TCP are deployed. These variants differ with respect to their congestion control and segment loss recovery techniques. The basic congestion control algorithms, namely *slow start*, *congestion avoidance*, and *fast retransmit*, were introduced in TCP Tahoe [18]. In TCP Reno [19], the *fast recovery* algorithm was added. This algorithm uses duplicate acknowledgements (ACKs) to trigger the transmission of new segments during the recovery phase, so that the network “pipe” does not empty following a fast retransmit. TCP NewReno introduced an *improved* fast recovery algorithm that can recover from multiple losses in a single window of data, avoiding many of the retransmission

timeout events that Reno experiences [13]. TCP’s selective acknowledgement (SACK) option was proposed to allow receivers to ACK out-of-order data [7]. With SACK TCP, a sender may recover from multiple losses more quickly than with NewReno. The aforementioned TCP variants use segment losses to estimate available bandwidth. TCP Vegas uses a novel congestion control mechanism that attempts to detect congestion in the network before segment loss occurs [5]. TCP Vegas, however, is not widely deployed on the Internet today.

Analytic modeling of TCP’s congestion-controlled throughput has received considerable attention in the literature (e.g., [2], [4], [6], [9], [16], [22], [23], [25], [27]–[29], [32], [35]–[37]). These analytical models have: (1) improved our understanding of the sensitivity of TCP to different network parameters; (2) provided insight useful for development of new congestion control algorithms for high bandwidth-delay networks and wireless networks; and (3) provided a means for controlling the sending rate of non-TCP flows such that network resources may be shared fairly with competing TCP flows. Most of these throughput models are based on TCP Reno [2], [6], [9], [16], [23], [25], [27]–[29], [32], while some models are based on SACK [36], [37], Vegas [35], and NewReno [22]. A detailed NewReno throughput model, however, seems missing from the literature.

This paper develops an analytic model for the throughput of a TCP NewReno bulk data transfer as a function of round-trip time (RTT) and loss rate. Our work is motivated, in part, by previous studies that indicate that TCP NewReno is widely deployed on the Internet [26], [30]. Furthermore, RFC 3782 indicates that NewReno is preferable to Reno, as NewReno provides better support for TCP peers without SACK [13].

Our TCP NewReno throughput model builds upon the well-known Reno model proposed by Padhye *et al.* [29], but differs from this PFTK model in three important ways. First, we explicitly model the fast recovery algorithm of TCP NewReno. In prior work [29], Reno’s fast recovery feature was not modeled. Depending on the segment loss characteristics, a NewReno flow may spend significant time in the fast recovery phase, sending per RTT an amount of data approximately equal to the slow start threshold. Second, we present an accurate formulation of NewReno’s timeout behaviour, including the possibility of incurring a timeout following an unsuccessful fast recovery. Third, our approach uses a two-parameter loss model that can model the loss event rate, as well as the burstiness of segment losses within a loss event. These two characteristics have orthogonal effects on TCP: a loss event triggers either fast recovery or a timeout, whereas the burstiness of losses affects the duration of the fast recovery period, and thus the performance of NewReno [31].

N. Parvez and C. Williamson are with the Department of Computer Science, University of Calgary, Canada. Email: {parvez, carey}@cpsc.ucalgary.ca
A. Mahanti is with National ICT Australia (NICTA), Eveleigh, NSW, Australia. Email: anirban.mahanti@nicta.com.au

Table I summarizes the Reno and NewReno models discussed in this paper. (The notation used is defined in Table II.) While some researchers believe that the PFTK model is adequate for modeling NewReno throughput, we show in this paper that this is not the case. In general, using the simple version of PFTK overestimates throughput, since timeouts are ignored, while (incorrectly) parameterizing the PFTK model with packet loss rate instead of loss event rate tends to underestimate throughput. In some cases, these two opposing errors offset each other, coincidentally leading to good predictions. As the Full TCP Reno model has been applied extensively in diverse areas, including TCP friendly rate control [12], [24], active queue management [8], and overlay bandwidth management [17], [21], we compare how accurately the Full Reno model estimates NewReno’s throughput. Our results show that the Full Reno model overestimates throughput for both Reno and NewReno bulk transfers. In general, we find that a detailed characterization of NewReno fast recovery behaviour, as provided in our model, is required to characterize NewReno throughput accurately.

We validated our model by conducting a comprehensive set of simulations using the *ns-2* simulator. In addition, we empirically validated our model by experimenting with the TCP NewReno implementation in the BSD TCP/IP protocol stack in an emulation environment, and with Internet experiments. Our results show that the proposed model can predict steady-state throughput of a TCP NewReno bulk data transfer for a wide range of network conditions.

Our TCP NewReno model also differs substantially from Kumar’s NewReno model [22]. First, Kumar’s model was developed for a local area network (LAN) environment and did not consider the effect of propagation delay on TCP throughput. Propagation delays cannot be ignored in environments such as the Internet, and our model explicitly considers RTT effects. Second, Kumar’s model, unlike the model presented in this paper, does not have a closed form. Specifically, throughput estimation using the Kumar model [22] requires use of numerical methods to compute the expected window size and the expected cycle time. In contrast, our model provides a simple closed form for throughput computation. The third (and probably the most significant) difference between the two models is with respect to the modeling of NewReno’s fast recovery behaviour. In Kumar’s work, the transmission of new segments and the duration of fast recovery are not explicitly modeled; his model considers only the probability of TCP transitioning to fast recovery. The improved fast recovery algorithm is NewReno’s key innovation with respect to its parent Reno, and we explicitly model TCP NewReno’s fast recovery behaviour in detail. In addition, our extensive simulation experiments demonstrate substantially greater throughput differences between Reno and NewReno (e.g., 30-50%) than in Kumar’s work. We do not present any comparisons with Kumar’s NewReno throughput model because that model was developed for a fundamentally different network environment (i.e., a LAN with negligible propagation delay, and a wireless link with random packet loss), and furthermore, has not been experimentally validated [22].

The remainder of this paper is organized as follows. Sec-

tion II presents an overview of NewReno’s fast recovery algorithm and our modeling assumptions. The proposed analytic model for TCP NewReno throughput is presented in Section III. The model is validated using simulations in Section IV, network emulations in Section V, and Internet experiments in Section VI. Section VII concludes the paper.

II. BACKGROUND AND ASSUMPTIONS

A. The NewReno Fast Recovery Algorithm

This section presents an overview of NewReno’s improved fast recovery algorithm [13]. All other congestion control components of NewReno, namely slow start, congestion avoidance, and fast retransmit, are identical to that of Reno. The reader is referred to references [19], [39], [40] for a detailed treatment of TCP Reno congestion control.

During congestion avoidance, receipt of four back-to-back identical ACKs (referred to as “triple duplicate ACKs”) causes the sender to perform fast retransmit and to enter fast recovery. In fast retransmit, the sender does the following:

- 1) retransmits the lost segment;
- 2) sets the slow start threshold $ssthresh$ to $cwnd/2$ (where $cwnd$ is the current congestion window size); and
- 3) sets $cwnd$ to $ssthresh$ (new) plus 3 segments.

In fast recovery (FR), the sender continues to increase the congestion window by one segment for each subsequent duplicate ACK received. The intuition behind the fast recovery algorithm is that these duplicate ACKs indicate that some segments are reaching the destination, and thus can be used to trigger new segment transmissions. The sender can transmit new segments if permitted by its congestion window.

In TCP Reno, receipt of a non-duplicate ACK results in *window deflation*: $cwnd$ is set to $ssthresh$ (i.e., the congestion window size in effect when the sender entered FR), FR terminates, and normal congestion avoidance behaviour resumes. When multiple segments are dropped from the same window of data, Reno may enter and leave FR several times, causing multiple reductions of the congestion window.

TCP NewReno modifies Reno’s FR behaviour on receipt of a non-duplicate ACK, by distinguishing between a “full” ACK (FA) and a “partial” ACK (PA). A full ACK acknowledges all segments that were outstanding at the start of FR, whereas a partial ACK acknowledges some but not all of this outstanding data. Unlike Reno, where a partial ACK terminates FR, NewReno retransmits the segment next in sequence based on the partial ACK, and reduces the congestion window by one less than the number of segments acknowledged¹ by the partial ACK. Thus NewReno recovers from multiple segment losses in the same window by retransmitting one lost segment per RTT, remaining in FR until a full ACK is received.

On receiving a full ACK, NewReno sets $cwnd$ to $ssthresh$, terminates FR, and resumes congestion avoidance.

¹This window reduction strategy is referred to as *partial window deflation*. In *full window deflation*, $cwnd$ is set to $ssthresh$ when partial ACKs are received. The current NewReno proposal in RFC 3782 recommends the partial window deflation option.

TABLE I
COMPARISON OF TCP THROUGHPUT MODELS (SEGMENTS PER ROUND TRIP TIME R)

Model	TCP Reno [29] (PFTK)	TCP NewReno	Details
Simple (NoTO)	$\frac{\sqrt{\frac{3}{2p}}}{R}$	$\frac{\frac{1}{p} + \frac{W^2 q}{1+Wq}}{(\frac{W}{2} + Wq + \frac{3}{2})R}$	Section III-A (Eq. 19)
Full Model	$\frac{1}{R\sqrt{(2p/3)+RTO} \min(1, 3\sqrt{(3p/8)})p(1+32p^2)}$	$\frac{\frac{1}{p} + \frac{W^2 q}{1+Wq}}{NR+pTO((1+2p+4p^2)RTO+(1+\log\frac{W}{4})R)}$, where $N = (\frac{W}{2} + \frac{3}{2} + (1-pTO)(1+Wq))$	Section III-B (Eq. 29)

B. Assumptions

This section outlines our assumptions regarding the application, the sender/receiver, and the network. Except for the segment loss model, all our assumptions are similar to those in prior work (e.g., [6], [16], [25], [29], [35], [36]).

1) *Application Layer*: Our model focuses on the steady-state throughput for *TCP bulk transfers*. We consider an application process that has an infinite amount of data to send from a source node to a destination node.

2) *TCP Sender and Receiver*: Our model assumes that the sender is using the TCP NewReno congestion control algorithm. The sender always transmits full-sized (i.e., MSS) segments whenever the congestion window allows it to do so. We assume that the sender is constrained only by the congestion window size, and not by the receiver's buffer size or advertised window. Also, the receiver sends one ACK for each received segment, and ACKs are never lost. These assumptions can be relaxed at the cost of somewhat more complex models using arguments similar to those in prior work [16], [29].

Similar to assumptions in other bulk transfer models [29], [35], our analysis ignores TCP's three-way connection establishment phase and initial slow start phase because the congestion avoidance algorithm dominates during a long-lived TCP bulk data transfer.

3) *Latency Model*: The latency of the TCP transfer is measured in terms of "rounds". The first round begins with the start of congestion avoidance; its duration is one RTT. All other rounds begin immediately after the previous round, and also last one RTT. The only exception is the round that terminates fast recovery and switches to congestion avoidance: its duration could be shorter than one RTT.

As in prior work [29], [35], we assume that the round duration is much larger than the time required to transmit segments in a round, and that the round duration is independent of the congestion window size. Segment transmission may be bursty or arbitrarily spaced within the round.

4) *Loss Model*: Our work introduces a novel two-parameter segment loss model that captures both the frequency of loss events and the burstiness of segment losses within a loss event. We define a loss event (LE) to begin with the first segment loss in a round that eventually causes TCP to transition from the congestion avoidance phase to either the fast recovery phase or the timeout phase.

For a congestion window size of W' , all losses within the next W' segments (starting from the first loss) are considered part of the same LE. This hierarchical relationship between an LE and losses within an LE is illustrated in Figure 1.

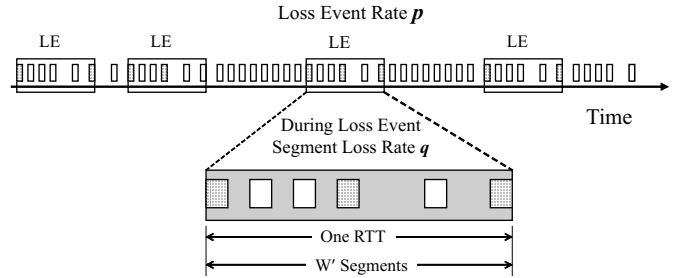


Fig. 1. The Two-Parameter Segment Loss Model

Note that an LE can start at any segment, but once it starts, it spans at most one RTT (equivalently, W'). The loss events are assumed to occur independently with probability p . Segments transmitted during an LE (except the first) are assumed to be lost independently with probability q (i.e., parameter q captures the "burstiness" of the segment losses within an LE). The two parameters can be set separately, to model either homogenous ($q = p$) or non-homogeneous ($q \neq p$) loss processes [41].

Many throughput models in the literature assume a restricted version of the foregoing loss model (e.g., [6], [16], [35], [36]). These models assume that following the first segment loss in a round, all subsequent segments transmitted in that round are lost. This assumption is appropriate for networks where packet losses occur from buffer overrun in DropTail queues; however, this assumption is inappropriate when packet losses occur because of active queue management policies or because of the characteristics of the transmission medium, as in the case of wireless networks.

Estimation of the two parameters p (the loss event rate) and q (the segment loss rate within a loss event) is specific to the application of the model. For example, for applications such as TCP friendly rate control of non-TCP flows [12], [24], the loss event rate p can be estimated using the Average Loss Interval (ALI) technique [12], which computes p as the inverse of the weighted average of the number of packets received (between loss events). Similar measurement-based approaches may be used to estimate q using non-invasive sampling [16]. Another practical option, discussed in Section IV-B, is to estimate q indirectly from the measured characteristics (e.g., loss event rate, overall packet loss rate).

III. THE ANALYTIC MODEL

This section develops the stochastic throughput model for TCP NewReno bulk data transfer. The model is developed in two steps. In Section III-A, the model is developed assuming

TABLE II
MODEL NOTATION

Parameter	Definition
p	Loss event rate
q	Segment loss rate within a loss event
R	Average round-trip time
<i>RTO</i>	Average duration of first timeout in a series of timeouts
W	Average of the peak congestion window size

that all loss events are identified by triple duplicate ACKs. Subsequently, in Section III-B, an enhanced model is developed that handles both triple duplicate ACKs and timeouts. The model notation is summarized in Table II.

A. Model without Timeout (NoTO)

In this section, we assume that all loss events are identified by triple duplicate ACKs, so that no timeouts occur. The model developed here is referred to as the “NoTO” model.

Ignoring the initial slow start phase, it follows from the arguments given in [29], [35] that the evolution of the congestion window can be viewed as a concatenation of statistically identical *cycles*, where each cycle consists of a congestion avoidance period, followed by detection of segment loss and a fast recovery period. Each of these cycles is called a Congestion Avoidance/Fast Recovery (CAFR) period.

The throughput of the flow can be computed by analyzing one such CAFR cycle. Let S_{CAFR} be the expected number of segments successfully transmitted during a CAFR period. Let D_{CAFR} denote the expected time duration of the period. Then the average throughput of the flow is:

$$T_{NoTO} = \frac{S_{CAFR}}{D_{CAFR}}. \quad (1)$$

Before determining the expectations of the variables in Equation 1, let us consider the illustration in Figure 2. Figure 2 shows the segment transmissions per round in two adjacent and identical CAFR periods. We focus on the i th such CAFR period, and use this example to illustrate the different events in a CAFR period. Each CAFR consists of congestion avoidance and fast recovery. The first round of a CAFR period corresponds to the start of congestion avoidance (marked I in Figure 2). During congestion avoidance, the congestion window opens linearly, increasing by one (vertically) the number of segments transmitted per round. We note that the time gap between two horizontally adjacent rectangles in the same CAFR period, on average, equals the RTT. In round $W/2 + 1 = 7$ in Figure 2, three (non-contiguous) transmitted segments are lost. The first of these lost segments (marked J in Figure 2) is detected in the following round upon receipt of triple duplicate ACKs, resulting in termination of congestion avoidance and a fast retransmit (marked N in Figure 2). TCP then enters fast recovery.

We use the term *drop window* to refer to the window’s worth of segments starting from the first lost segment in round $W/2 + 1$ to the segment transmitted just before the receipt of the first duplicate ACK. Suppose that m segments are lost in the drop window. As shown in Figure 2 (and Figure 3),

fast recovery continues for m RTTs with TCP sending up to approximately $W/2$ new segments per RTT. TCP exits fast recovery and resumes normal congestion avoidance behaviour when a full ACK (FA) is received.

From our assumptions regarding statistically identical CAFR periods, we extrapolate and consider the case where two adjacent CAFR periods are exactly identical, as shown for example in Figure 2. From Figure 2 we see that S_{CAFR} can be expressed as the sum of: 1) the expected number of segments α transmitted between the end of one LE and the start of the next LE (e.g., between D and J in Figure 2); and 2) the expected number of segments δ transmitted between the first loss and the last loss (e.g., between J and L in Figure 2) of a loss event. It follows from the assumptions regarding loss events that the expected value of α is $1/p$ [29], [35]. Therefore,

$$S_{CAFR} = \frac{1}{p} + \delta. \quad (2)$$

Next, we derive δ . For m uniformly spaced drops in a typical window of size W , the expected number of segments transmitted between the first and the last loss in the same CAFR period (e.g., between J and L in Figure 2) is:

$$\delta \approx W - WE \left[\frac{1}{m} \right] \approx W - \frac{W}{E[m]} \quad (3)$$

The expected value of m can be obtained as follows. Let $A(W, m)$ denote the probability of m segment losses from a drop window of size W . By definition, the first segment in the drop window is always lost. Because segments are lost independently of other segments, the probability that $m - 1$ segments are lost from the remaining $W - 1$ segments in the window follows the Binomial probability mass function. Therefore,

$$A(W, m) = C_{m-1}^{W-1} (1 - q)^{W-m} q^{m-1}, \quad (4)$$

where C_{m-1}^{W-1} represents the binomial coefficient.

Since we have assumed that all losses are identifiable by triple duplicate ACKs, we know that $m \leq W - 3$. Hence²,

$$E[m] = \sum_{m=1}^{W-3} mA(W, m) \approx 1 + (W - 1)q \approx 1 + Wq. \quad (5)$$

Substituting $E[m]$ into Equation 3, we obtain:

$$\delta = \frac{W^2q}{1 + Wq}. \quad (6)$$

Finally, substituting δ into Equation 2 we obtain:

$$S_{CAFR} = \frac{1}{p} + \frac{W^2q}{1 + Wq}. \quad (7)$$

To compute W in terms of p and q , we need an alternate expression for S_{CAFR} . From Figure 2, note that S_{CAFR} can be expressed as the sum of: 1) the expected number of segments S_{LI} transmitted in the linear increase phase (from round 1 to round $W/2 + 1$); 2) the expected number of segments S_{β} transmitted from the start of round $W/2 + 2$

²This approximation assumes q is small. All subsequent approximations also assume that q is small.

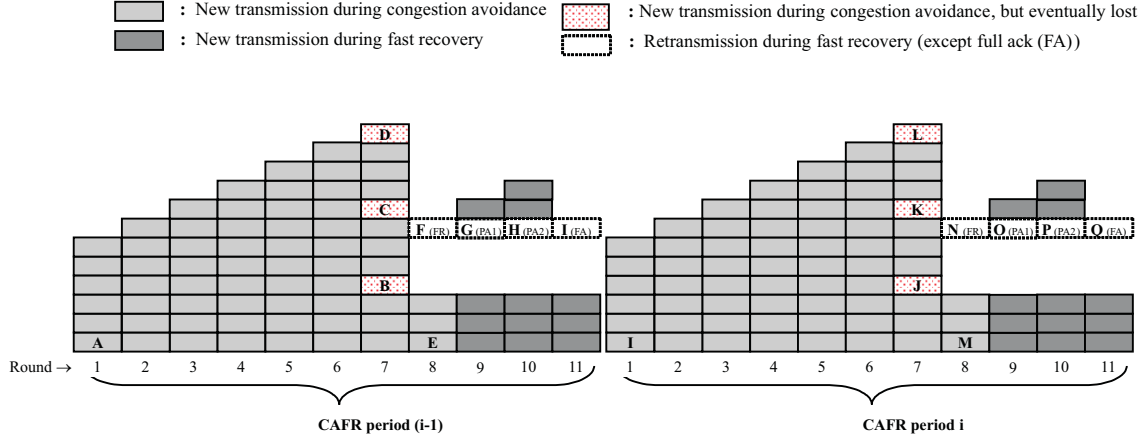


Fig. 2. Segment Transmissions in Two Adjacent and Identical CAFR Periods

(marked M in Figure 2) until triple duplicate ACKs terminate congestion avoidance (N in Figure 2); and 3) the expected number of segments S_{FR} transmitted during fast recovery (from N to Q in Figure 2). Therefore,

$$S_{CAFR} = S_{LI} + S_{\beta} + S_{FR}. \quad (8)$$

We will determine S_{FR} first. The time view of a CAFR period shown in Figure 3 may be helpful in following the ensuing discussion. When TCP detects a segment loss and enters fast recovery, the expected number of outstanding segments is W . With m drops from the window, the source receives $W - m$ duplicate ACKs during the first RTT of fast recovery. Each duplicate ACK increases the congestion window by one segment, so at the end of the first RTT the congestion window size will be $\frac{3}{2}W - m$. This inflated congestion window allows TCP to send $\frac{W}{2} - m$ new segments during the first RTT of fast recovery, provided $m \leq \frac{W}{2}$. The second RTT starts with the reception of the first partial ACK (PA1). Immediately following the receipt of the partial ACK, TCP retransmits the next lost segment and also transmits one new segment. During this second RTT of fast recovery, $\frac{W}{2} - m$ additional duplicate ACKs will arrive, increasing the congestion window size by the same amount. This window increase allows the transmission of $\frac{W}{2} - m$ new segments as well. In total, TCP transmits $\frac{W}{2} - m + 1$ segments in the second RTT. For m segment losses, fast recovery requires exactly m round-trip times to recover all the lost segments with TCP transmitting $\frac{W}{2} - m + j - 1$ new segments in the j th RTT of fast recovery. Generalizing we obtain:

$$S_{FR}^{m \leq \frac{W}{2}} = \sum_{j=1}^m \left(\frac{W}{2} - m + j - 1 \right) = \frac{m}{2} (W - m - 1). \quad (9)$$

If $m > \frac{W}{2}$, TCP will not transmit any new data during the first RTT of fast recovery, because the congestion window size $\frac{3}{2}W - m$ at this time is smaller than the amount of outstanding data W . With each partial ACK, the congestion window size increases by one segment. Thus, TCP needs $m - \frac{W}{2}$ partial ACKs to inflate the congestion window size to the number of outstanding segments W . Therefore, on arrival of the $(m - \frac{W}{2} + 1)$ th partial ACK, TCP can transmit one new segment.

In the next RTT, TCP will transmit two new segments, and so on. In general:

$$S_{FR}^{m > \frac{W}{2}} = \sum_{k=m - \frac{W}{2} + 1}^{m-1} \left(\frac{W}{2} - m + k \right) = \frac{W^2}{8} - \frac{W}{4}. \quad (10)$$

Using Equations 4, 9, and 10, the expected number of new segments transmitted during fast recovery is:

$$S_{FR} = \sum_{m=1}^{\frac{W}{2}} A(W, m) S_{FR}^{m \leq \frac{W}{2}} + \sum_{m=\frac{W}{2}+1}^{W-3} A(W, m) S_{FR}^{m > \frac{W}{2}} \\ \approx \frac{W^2}{2} (q - q^2) + \frac{W}{2} (1 - 5q + 3q^2) - (1 - 2q + q^2). \quad (11)$$

We next determine S_{LI} for Equation 8. Immediately following receipt of a full ACK, fast recovery is terminated and the congestion window is reset to $W/2$ (e.g., I in Figure 2). This also ends the current cycle and normal congestion avoidance begins. In this phase, the congestion window increases by one segment per round until it reaches the assumed peak value of W in round $W/2 + 1$. It therefore follows that:

$$S_{LI} = \sum_{i=\frac{W}{2}}^W i = \frac{3}{8}W^2 + \frac{3}{4}W. \quad (12)$$

To determine S_{β} for Equation 8, we consider its two extreme boundary cases. If the first loss occurs at the start of round $W/2 + 1$, then the number of segments S'_{β} transmitted in the next round until termination of congestion avoidance is 0. Similarly, $S'_{\beta} = W - 1$ if the first loss occurs at the end of round $W/2 + 1$. Therefore, we approximate³ S_{β} with its median value $W/2$.

Substituting the expressions for S_{LI} , S_{FR} , and S_{β} into Equation 8 and simplifying, we obtain:

$$S_{CAFR} = \left(\frac{3}{8} + \frac{q}{2} - \frac{q^2}{2} \right) W^2 + \left(\frac{7}{4} - \frac{5q}{2} + \frac{3q^2}{2} \right) W - (1 - 2q + q^2) \quad (13)$$

³This approximation introduces a small amount of error into our model.

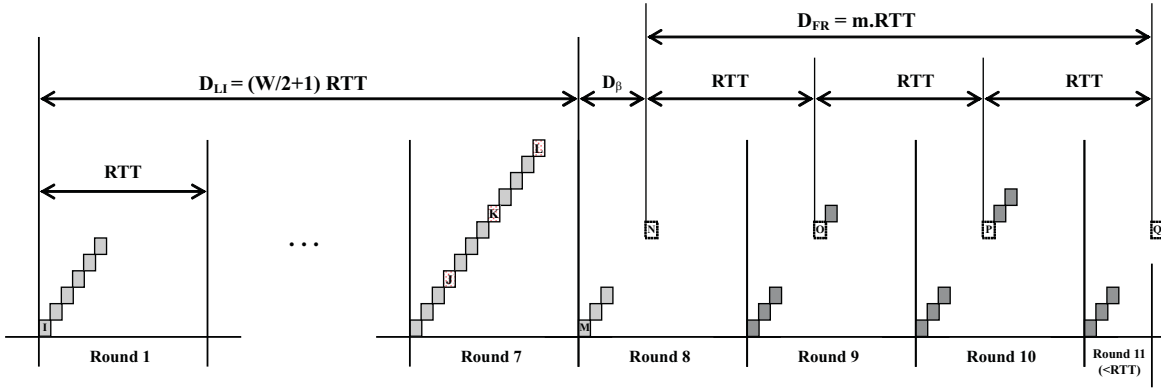


Fig. 3. Time View of a CAFR Period

Equating the right-hand sides of Equation 7 and Equation 13, and neglecting high-order terms, we can express the value of W in terms of p and q as:

$$W \approx \frac{10pq - 5p + \sqrt{p(24 + 32q + 49p)}}{p(3 + 4q)}. \quad (14)$$

Equation 14 encapsulates the essential characteristics of our two-parameter loss model, which are illustrated graphically in Figure 4. When p is very small, W is large, but decreases as q is increased (i.e., fast recovery takes longer, and is less likely to succeed). As p increases, W decreases, and q has a negligible impact, since fast recovery is rarely applicable.

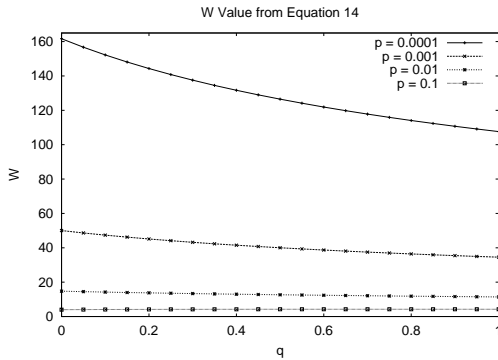


Fig. 4. Effect of p and q on Window Value W

To obtain the expected time duration of a CAFR period, we again refer to the time view of a CAFR period, shown in Figure 3. From this illustration, we note that:

$$D_{CAFR} = D_{LI} + D_{\beta} + D_{FR}, \quad (15)$$

where D_{LI} is the expected duration of a linear increase period, D_{β} is the expected delay from the start of round $(W/2+2)$ to the end of congestion avoidance, and D_{FR} is the expected duration of the fast recovery phase. The duration of the linear increase phase is:

$$D_{LI} = \left(\frac{W}{2} + 1 \right) R. \quad (16)$$

For m segment losses in the drop window, fast recovery requires m round-trip times. Therefore,

$$D_{FR} = E[m]R \approx (1 + Wq)R \quad (17)$$

Using arguments similar to those used for determining S_{β} , we approximate using $D_{\beta} = \frac{R}{2}$. Substituting D_{LI} , D_{β} , and D_{FR} into Equation 15, we obtain:

$$D_{CAFR} = \left(\frac{W}{2} + Wq + \frac{5}{2} \right) R \quad (18)$$

Finally, substituting Equation 7 and Equation 18 into Equation 1, we obtain:

$$T_{NoTO} = \frac{\frac{1}{p} + \frac{W^2q}{1+Wq}}{\left(\frac{W}{2} + Wq + \frac{5}{2} \right) R}, \quad (19)$$

where W can be computed from Equation 14.

B. Full Model (Full)

This section extends the foregoing model to include timeouts as loss indications. We refer to this as the ‘‘Full’’ model.

We again view the congestion window evolution as a concatenation of statistically identical cycles. Each cycle consists of several CAFR periods followed by a CATOSS period, where a CATOSS period is the concatenation of congestion avoidance (CA), timeout (TO), and slow start (SS) periods, as shown in Figure 5. Therefore, the throughput of a TCP NewReno flow can be expressed⁴ as:

$$T_{Full} = \frac{(1 - p_{TO})S_{CAFR} + p_{TO}(S_{CA} + S_{TO} + S_{SS})}{(1 - p_{TO})D_{CAFR} + p_{TO}(D_{CA} + D_{TO} + D_{SS})} \quad (20)$$

where p_{TO} is the probability that a loss event leads to a timeout. S_X is the expected number of successful segment transmissions in a period of type X , and D_X is the expected duration of a period of type X . Obviously, $D_{CA} = D_{LI} + D_{\beta}$. Intuitively, $S_{CA} = S_{LI} + S_{\beta}$. However, we use $S_{CA} = S_{LI}$ instead, since TCP forgets outstanding data after timeout.

TCP NewReno may experience a timeout either from the congestion avoidance phase or from the fast recovery phase. The former transition occurs when TCP does not receive

⁴This expression ignores the duration of an incomplete fast recovery phase, as well as any new segments transmitted therein.

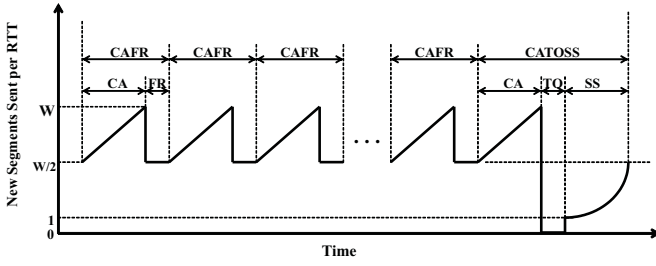


Fig. 5. Segment Transmissions in a Cycle (multiple CAFRs followed by CATOSS)

enough duplicate ACKs to trigger fast retransmit/fast recovery, while the latter transition occurs when retransmitted segments are lost during the fast recovery phase. We express p_{TO} as:

$$p_{TO} = p_{D_{TO}} + p_{IFR} \quad (21)$$

where $p_{D_{TO}}$ is the probability of directly transitioning to timeout from congestion avoidance and p_{IFR} is the probability of a timeout due to an unsuccessful fast recovery.

We determine $p_{D_{TO}}$ as follows. TCP experiences direct timeout when more than $W - 3$ segments are lost from a drop window of size W . Recalling the definition of $A(W, m)$ in Equation 4, we get:

$$p_{D_{TO}} = \sum_{m=W-2}^W A(W, m). \quad (22)$$

When TCP NewReno loses no more than $W - 3$ segments from a drop window of size W , it enters fast recovery. On entering fast recovery, a timeout will occur if any segments retransmitted during fast recovery are lost. We approximate this condition by assuming that if a new loss event occurs during fast recovery, then the segment retransmitted in that RTT of fast recovery is also lost, thus triggering timeout. (While we do not explicitly model successive occurrences of FR, this assumption implicitly captures its effect by increasing the probability of timeout.) For m losses in the drop window, NewReno needs m round-trip times, sending approximately $W/2$ segments (including retransmissions) per RTT. The probability that the i th segment is lost given that the previous $i - 1$ segments arrived at the destination is $(1 - p)^{i-1}p$. Therefore, it follows from our assumptions that:

$$\begin{aligned} p_{IFR} &= \sum_{m=1}^{W-3} A(W, m) \left[p + (1-p)p + \dots + (1-p)^{\frac{mW}{2}-1}p \right] \\ &= \sum_{m=1}^{W-3} A(W, m) \left[1 - (1-p)^{\frac{mW}{2}} \right]. \end{aligned} \quad (23)$$

Substituting Equations 22 and 23 in Equation 21, we get:

$$p_{TO} = 1 - \sum_{m=1}^{W-3} A(W, m) \left[(1-p)^{\frac{mW}{2}} \right]. \quad (24)$$

Derivation of the expected duration of timeout is similar to [29]. Furthermore, during timeout TCP does not transmit

any new segments. Thus,

$$S_{TO} = 0 \quad \text{and} \quad (25)$$

$$D_{TO} = RTT \frac{1+p+2p^2+4p^3+8p^4+16p^5+32p^6}{1-p}. \quad (26)$$

In the slow start phase, the initial window size is 1 and the window size is doubled every round until the slow start threshold ($W/2$) is reached. In the last round of slow start, TCP transmits $W/2$ segments and enters congestion avoidance. We count the duration and segments of the last round of slow start as being part of congestion avoidance. Hence,

$$S_{SS} = 1 + 2 + 4 + \dots + \frac{W}{4} = 2^{1+\log \frac{W}{4}} - 1 \quad \text{and} \quad (27)$$

$$D_{SS} = \left(\log \frac{W}{4} + 1 \right) R. \quad (28)$$

Following the approach in [35], we can replace the numerator of Equation 20 with $\frac{1}{p} + \frac{W^2q}{1+Wq}$. Substituting Equations 18, 26, 28, and D_{CA} into Equation 20, we obtain:

$$T_{Full} = \frac{\frac{1}{p} + \frac{W^2q}{1+Wq}}{NR + p_{TO} \left((1+2p+4p^2)RTT + (1+\log \frac{W}{4})R \right)}, \quad (29)$$

where $N = \left(\frac{W}{2} + \frac{3}{2} + (1 - p_{TO})(1 + Wq) \right)$, and W can be computed from Equation 14.

To apply this model, the user should obtain the loss event rate p , packet loss rate \tilde{q} , and round-trip time R . The ratio of \tilde{q} to p determines m , and then the value of q in the model can be computed using Equation 5. (Also see Section IV-B and Equation 30.)

IV. MODEL VALIDATION

This section validates the proposed NewReno throughput model using the *ns-2* network simulator⁵. The results reported here also illustrate the performance advantages of NewReno over Reno. Finally, we quantify the ineffectiveness of existing TCP Reno models in predicting TCP NewReno throughput.

A. Network Model and Traffic Models

Before discussing the simulation results, we present the basic setup used in the *ns-2* simulations. Specifically, we describe the network model and the various traffic models used. To conserve space when presenting the results, we describe only the setup changes with respect to the default settings discussed here.

The results reported here, with the exception of those in Section IV-E, are for a simple dumbbell network topology with a single common bottleneck between all sources and sinks. Each source/sink pair is connected to the bottleneck link via a high bandwidth access link. The propagation delays of the access links are varied to simulate the desired round-trip delay between a source/sink pair. We refer to the flows that are being actively monitored as the “foreground” flows, with all other traffic designated as “background” flows.

All experiments have two long duration foreground flows: one NewReno flow and one Reno flow. These long duration flows simulate the bulk data transfer sessions of interest. The receive buffers for the foreground flows are sufficiently

⁵<http://www.isi.edu/nsnam/ns>.

provisioned such that their buffer space advertisements do not limit the congestion window size. The experiments vary the bottleneck bandwidths (e.g., 15 Mbps to 60 Mbps), the round-trip delays of the flows (e.g., 20 ms to 460 ms), the bottleneck queue management policies (e.g., DropTail and RED), and the load/mix of background traffic (e.g., mix of long duration FTP transfers, short duration HTTP sessions, and constant bit rate UDP flows). For RED queue management, the *minthresh* and the *maxthresh* are set to 1/3 and 2/3 of the corresponding queue size limit, based on recommendations in Section 6 of [11].⁶

Background HTTP traffic is simulated using a model similar to that in [24], [35]. Specifically, each HTTP session consists of a unique client/server pair. The client sends a single request packet across the (reverse) bottleneck link to its dedicated server. The server, upon receiving the request, uses TCP to send the file to the client. Upon completion of the data transfer, the client waits for a period of time before issuing the next request. These waiting times are exponentially distributed and have a mean of 500 ms. The file sizes are drawn from a Pareto distribution with mean 48 KB and shape 1.2 to simulate the observed heavy-tailed nature of HTTP transfers [3].

Background HTTP and FTP sessions use TCP NewReno with a maximum congestion window size of 64 KB. The packet size is 1 KB. All packets are of identical size except HTTP request packets and possibly the last packet of each HTTP response. The round-trip propagation delays of these background flows are uniformly distributed between 20 ms and 460 ms, consistent with measurements reported in the literature [1], [20].

The background UDP flows are constant bit rate UDP flows with rate 1 Mbps each. The packet size is 1 KB and the one-way propagation delay for each UDP flow is 35 ms.

The results reported here are for the “Full” TCP NewReno model, unless stated otherwise. As a representative TCP Reno throughput model, we use the full PFTK model from Table I, which has similar modeling assumptions [29]. This TCP Reno throughput model has been widely used in prior work (e.g., [12], [17], [21], [24]).

The necessary input parameters for both analytical models are obtained from the simulation trace file. All the losses in a single window of data are counted as one loss event. The loss event rate p is taken to be the ratio of the total number of loss events to the total number of segment transmissions, in the period of interest. For simplicity, we assume a homogeneous loss process ($q = p$), unless stated otherwise. The average round-trip time R was measured at the sender, and RTO was approximated as $3R$.

In simulations where multiple long duration flows share a single bottleneck link, systematic discrimination has been observed against some connections [14], [15]. Such *phase* effects, however, rarely arise in experiments that consider a mix of long and short duration flows, with heterogeneous round-trip propagation delays [15]. As a precautionary measure, the experiments reported here start all flows at slightly different

times. The background flows start at uniformly distributed times between 0 and 2 seconds, and the foreground flows start at uniformly distributed times between 5 and 7 seconds, all measured in simulation time since the start of a run. Each experiment simulates 1000 seconds of run. Results are reported using data from the last 750 simulated seconds.

B. Bursty Loss Model

Our first experiment illustrates the flexibility of our novel two-parameter loss model, and the key differences between our NewReno model and the PFTK model. The simulation results reported here are for a *single* foreground NewReno flow traversing a 45 Mbps bottleneck link. No background flows are present, and the round-trip propagation delay of the NewReno flow is 75 ms. A specialized drop module that takes as input two parameters p and m was placed on the access link of the TCP Sink node. This drop module schedules Bernoulli loss events at rate p ; whenever a loss event occurs, m back-to-back packets are dropped.

We first develop an approximation for computing q from the measured characteristics of the flow. Given the average loss rate \tilde{q} observed over the entire duration of the transfer, and the loss event rate p , a relation between \tilde{q} , q , p , and W can be obtained as follows. The expected number of segment losses per loss event is $m = \tilde{q}/p$. Using Equation 5, we obtain:

$$q \approx \frac{\tilde{q}/p - 1}{W - 1}, \quad (30)$$

where W is computed from Equation 14 using $q = \tilde{q}$.

Figure 6(a) shows the simulation throughput for the NewReno flow, along with the results from the analytic model. In the experiments, m was varied from 1 to 20 while keeping the loss event rate fixed at 0.05%. The analytic results are shown for the full NewReno model, with q approximated using Equation 30. When the loss event rate is low (0.05%), and there is a single packet loss per loss event, the results from the NewReno model and the PFTK model are similar. As the number of packet drops m per loss event increases, the simulated NewReno throughput decreases roughly linearly, since the duration of fast recovery is proportional to the number of drops. Our model tracks this trend well, while the PFTK model does not consider the number of packet drops⁷ per loss event.

Figure 6(b) shows similar results for a higher loss event rate. The value of m was varied from 1 to 10, while keeping the loss event rate fixed at 1.0%. These results show even greater differences between the NewReno model and the PFTK model. As the loss event rate increases, or as the number of packet drops per loss event increases, the simulated NewReno throughput decreases significantly compared to that predicted by the PFTK model, while our NewReno model follows the downward trend well.

These results demonstrate the accuracy and robustness of our analytic model. The two-parameter loss model is particularly useful in scenarios that involve bursty packet losses. In

⁶While the difficulties of setting RED parameters are well-documented in the literature, our modeling results are consistent for other reasonable settings of RED parameters.

⁷In Figure 6, we used the loss event rate p to parameterize the PFTK model. Using the packet loss rate mp makes the prediction error even worse.

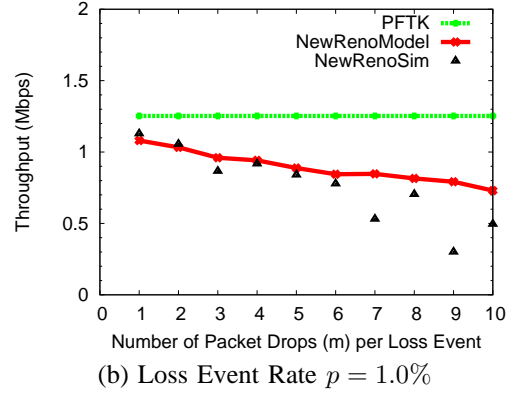
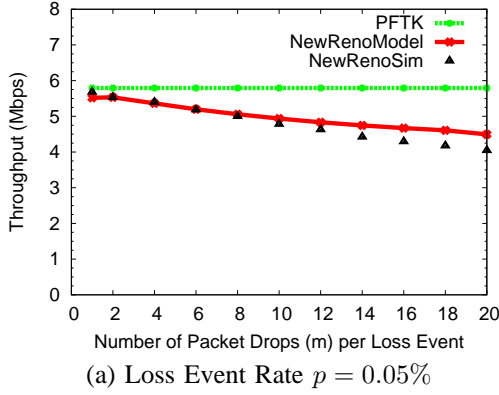


Fig. 6. Model Accuracy with Bursty Packet Losses)

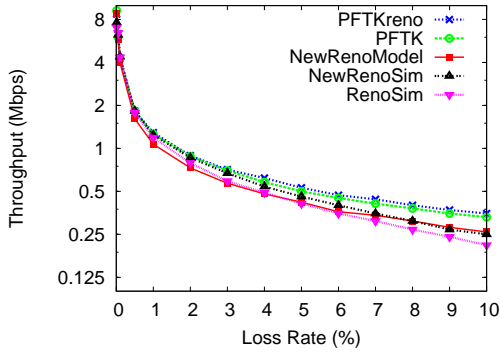


Fig. 7. Model Throughput Accuracy (log scale) with Bernoulli Packet Loss

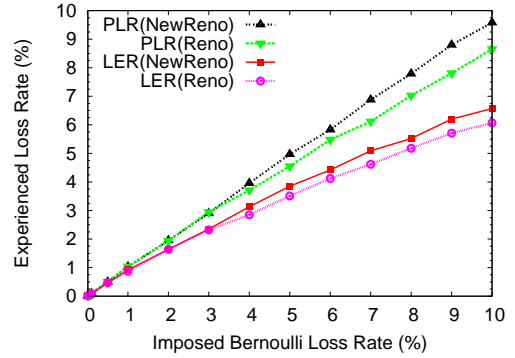


Fig. 8. Packet Loss Rate (PLR) and Loss Event Rate (LER) for the Imposed Bernoulli Loss Rate

a separate paper [31], we use the q parameter (and a fixed loss event rate p) to study the effect of bursty packet losses on two variants of NewReno, namely Slow-but-Steady (SBS) and Impatient (IMP). Contrary to RFC 3782, we find that the SBS variant offers superior throughput to IMP in all but the most extreme packet loss scenarios (e.g., 26 or more segment losses per window [31]). Similar experiments (not shown here) clearly demonstrate the superiority of partial window deflation versus full window deflation in TCP NewReno. These insights were made possible by the two-parameter loss model.

C. Bernoulli Packet Loss

Before validating the model with background traffic, validation is carried out in isolation. The configuration considered here consists of *two* foreground flows traversing a 15 Mbps bottleneck link. A Bernoulli packet drop module was placed on the access link of each foreground flow. The bottleneck router's buffer was sufficiently provisioned such that there were no congestion-induced packet losses. Experiments varied the imposed Bernoulli packet loss rate from 0.01% to 10%.

Figure 7 shows the throughput from the simulations and the models from representative experiments with round-trip propagation delay of the foreground flows set to 75 ms. For the imposed Bernoulli loss rates, the corresponding observed loss event rates (LER) and packet (segment) loss rates (PLR) for both foreground flows are shown in Figure 8.

Several important observations are evident from the results in Figure 7. The results show that the proposed NewReno throughput model (NewRenoModel in the figures) is able to track accurately the simulation throughput over the entire range of loss rates considered. The prediction error of our model, defined as $|simulation - model|/simulation$, ranges from 0% to 15% with an average error of 9.0%. Furthermore, if the PFTK model (PFTK in the figure) is naively used to estimate NewReno throughput (based on the loss event rate experienced by the foreground NewReno flow), the prediction errors range from 0% to 32%, with an average absolute prediction error of 11%.

The PFTK model is poor at predicting the simulated Reno throughput (PFTKreno in the figures, based on the observed loss event rate for the foreground Reno flow), especially at high loss rates. At high loss rates, multiple packet losses per window are possible, leading to multiple window reductions, or even timeout. The PFTK model essentially considers a single drop per loss event, and is thus unable to predict the throughput accurately. The average prediction error is 25%.

The higher prediction errors in the PFTK model can be attributed to the omission of the Reno fast recovery algorithm from their model, and the correlated packet loss assumptions of their model. Note that with the Bernoulli packet drop module, most packet losses are isolated single packet drops that can be recovered using a single fast recovery phase. For low packet loss rates (e.g., 2% or lower), the throughputs for simulated

Reno and NewReno flows are thus similar (because of the Bernoulli packet loss assumption).

D. HTTP/FTP Background Traffic

The simulation results reported in this section are for a 15 Mbps bottleneck link with a queue of capacity 150 packets. In order to investigate the effect of varying degrees of multiplexing, the total number of background flows is varied from 100 to 200, using a mix of 75% HTTP and 25% FTP flows. Both foreground flows have a round-trip propagation delay of 75 ms.

Figure 9 shows the simulated throughputs of NewReno and Reno as well as the throughputs from the analytic models. Figure 9(a) is for a DropTail bottleneck router, while Figure 9(b) is for a RED bottleneck router. The simulation results in Figure 9(a) show that NewReno throughput is often 20-30% higher than that of Reno. This is because the cross traffic generates bursty packet losses at the DropTail router buffer. NewReno is able to recover efficiently from these losses using its improved fast recovery algorithm. The performance differences between Reno and NewReno decrease when RED queues are used, as can be seen in Figure 9(b). The overall throughput with RED is slightly lower as well.

From Figure 9, we also note that the proposed analytic model tracks the throughput of the foreground flow for the range of background traffic considered. The prediction error of our analytic model averages 4.4% with DropTail queues, and 8.9% for the RED queue management policy.

The results also show that the PFTK model overestimates both Reno and NewReno throughputs. The average prediction error is 20% with DropTail queues, due to the bursty losses induced by the HTTP workload. However, the average prediction error for RED queues (9.9%) is lower. With RED queues, the burstiness of packet losses decreases, allowing some of the packet losses to be recovered by the Reno fast recovery algorithm. The PFTK model essentially captures a single packet loss per loss event, though it assumes that packet losses are correlated within a round. While the PFTK model is intended for bottleneck routers with DropTail queue management, rather than those with active queue management, the PFTK model has been applied in the latter context by others [9], [30].

Our results indicate that our NewReno model provides relatively robust results for both DropTail and RED packet loss scenarios. We have also shown that the PFTK model is inadequate for modeling NewReno throughput, especially when the bottleneck link is shared by many bursty flows.

E. Multiple Bottlenecks

This section reports validation results from an experiment setup with multiple bottlenecks. The network topology used here consists of two dumbbell networks connected in series at the bottlenecks. Each bottleneck link had a capacity of 15 Mbps with a buffer space for 150 packets. Two long duration TCP flows, one NewReno and one Reno, traversed both bottleneck links. The foreground flows had a round-trip propagation delay of 75 ms. Background traffic was applied to

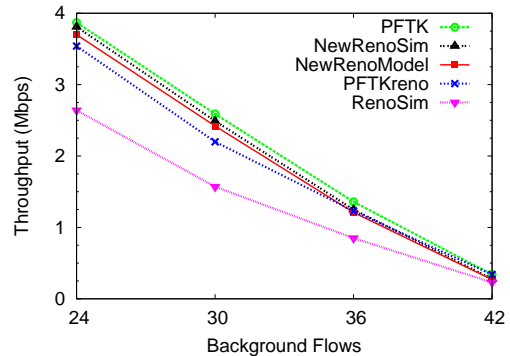


Fig. 11. Model Accuracy with Background UDP Traffic

the bottleneck links such that each background flow traversed only a single bottleneck link. Specifically, each bottleneck link experienced background traffic mix that consisted of 75% HTTP flows and 25% FTP flows. We varied the total number of flows per bottleneck from 100 to 200.

Note that although statistically identical background load is simulated on each bottleneck link, randomness in the HTTP traffic generation process can result in slightly different (and time-varying) background loads on the bottleneck links. It is also noteworthy that the foreground flows may experience losses at *both* bottleneck links, and thus the results presented here are not directly comparable to those for the experiments with a single bottleneck link.

Figure 10 shows the throughput from the simulations and the results from the analytic models. As shown in Figure 10, our NewReno throughput model closely tracks the simulation throughput over the entire range of background load simulated. The average prediction error in these experiments is 3.4%.

Compared to the DropTail experiment results, the results from the experiments with RED queues show somewhat higher prediction errors. The prediction errors in this setting average 7.5%. We note that the NewReno flow experienced slightly higher packet loss in the RED experiments.

Similar to earlier results, we observe that the prediction errors increase significantly if the PFTK model is used to estimate NewReno throughput. In the multiple bottleneck experiments, the average prediction error of the PFTK model (when tracking NewReno throughput) is 25% for DropTail routers and 27% for RED queue management. The inaccuracy of the PFTK model arises from its failure to consider the number of packet drops per loss event. Our model accurately captures the effect of multiple drops on the duration of the fast recovery period.

F. UDP Background Traffic

This section considers the impact of background traffic that is predominantly generated by On-Off Constant Bit Rate (CBR) UDP flows. The experiments reported here are for a 15 Mbps bottleneck link with a queue limit of 150 packets. The background traffic consists of a fixed number of HTTP/FTP background flows (24 HTTP sessions and 8 FTP sessions), and a varying number of On-Off CBR UDP flows, whose On and Off times are drawn from a heavy-tailed Pareto distribution

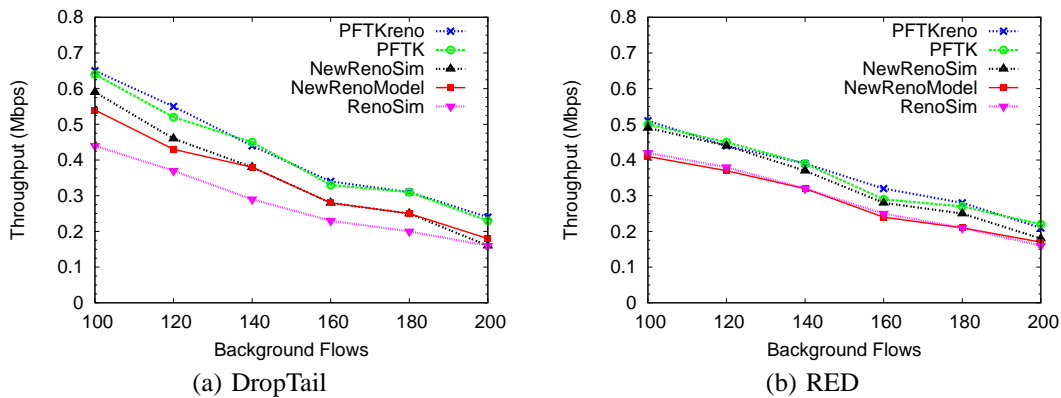


Fig. 9. Model Accuracy with Background HTTP/FTP Traffic

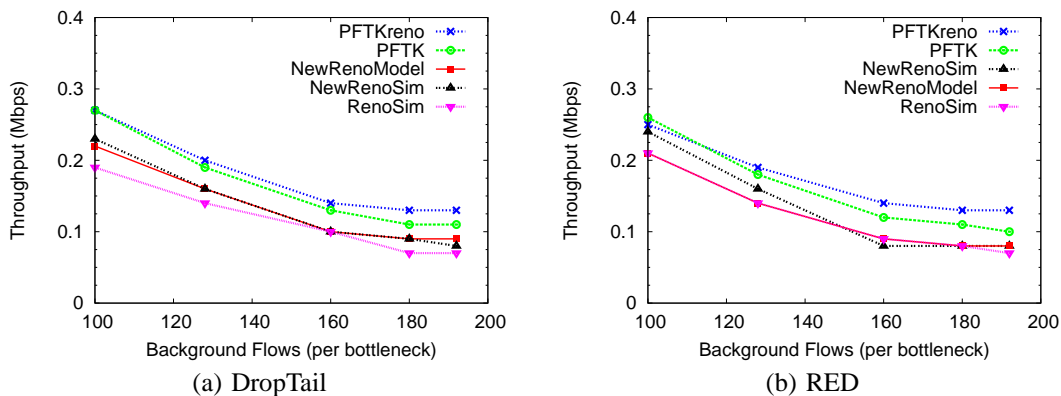


Fig. 10. Model Accuracy with Multiple Bottlenecks

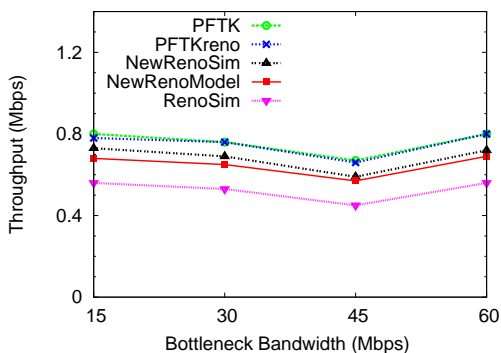


Fig. 12. Model Accuracy with System Scaling

with 1.2 as the shape parameter. The two foreground flows, namely NewReno and Reno, each have a round-trip propagation delay of 75 ms.

The results in Figure 11 again show that TCP NewReno can significantly outperform TCP Reno under similar network conditions. We also observe that the proposed analytic model closely tracks NewReno throughput, with an average prediction error of 3.1% in the DropTail experiments. Similar to the results reported in the earlier sections, the PFTK model has higher prediction error (9.0%). For RED queues (not shown here), the two models produce comparable results, each with an average prediction error below 10%.

G. System Scaling

The next experiment studies the robustness of our model to the scaling of network model and workload parameters.

Figure 12 shows the simulated throughput of the foreground flows and the results from the analytic models for a range of bottleneck bandwidths. Here, the initial experimental setup had a 15 Mbps bottleneck link with a buffer of 50 packets and 100 background flows. The background flows consist of 10% FTP flows and 90% HTTP sessions. At each step, all system resources and the background loads are scaled upwards. Thus, for each new configuration, the bottleneck capacity is increased by 15 Mbps, the queue size by 50 packets, and the number of background flows by 100 (90 HTTP sessions and 10 FTP sessions). The foreground NewReno and Reno flows each have a round-trip propagation delay of 75 ms.

The simulation results show that NewReno throughput is typically 20-35% higher than Reno throughput under identical network conditions. It can be observed that our NewReno analytic model accurately tracks the throughput observed in the simulations for a wide range of bandwidths. The average prediction error of the NewReno model is 5.1%. Similar to observations made in earlier sections, predicting NewReno throughput with the PFTK throughput model has higher prediction errors (e.g., an average prediction error of 11%). The average prediction error of PFTK for Reno throughput is 17%.

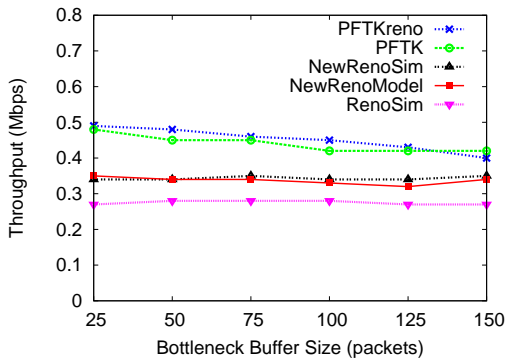


Fig. 13. Model Accuracy with Varying Buffer Size

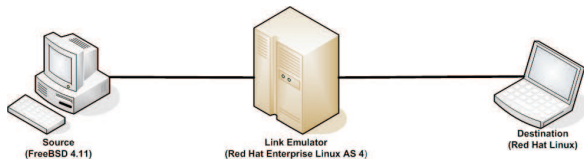


Fig. 14. Testbed for Emulation Experiments

H. Bottleneck Buffer Size

The next experiment tests the sensitivity to the bottleneck buffer size, which affects the overall packet loss rate as well as the burstiness of packet losses. In this experiment, we set the number of background flows to 100, with 50 FTP flows and 50 HTTP flows. The bottleneck buffer is changed from 25 packets to 150 packets in increments of 25. The other simulation parameters are kept identical to the experiments in Section IV-D.

Figure 13 shows the throughput results along with model predictions for the different buffer sizes. The NewReno model tracks the simulation throughput reasonably well, with an average prediction error of 2.9%. The PFTK model prediction for NewReno throughput is poor, with an average prediction error of 28%. The accuracy of our model stems from its careful consideration of the fast recovery process for bursty losses. As in other cases with bursty packet losses, the PFTK model overestimates the throughput, since it implicitly assumes that all losses are recoverable within a simple fast recovery period that lasts only a single RTT (assuming a timeout does not occur).

This experiment reinforces the generalized observations made in Section IV-B, and shows that the proposed NewReno model provides more robust throughput predictions than PFTK when congestion loss dominates.

V. EMULATION EXPERIMENTS

We validated our TCP NewReno throughput model using a real TCP source and a real TCP sink on an emulated wide area network in our laboratory. This section describes the experimental testbed used for emulation, the emulated network configuration, and the experimental results.

A. Testbed Configuration

The testbed consists of three physical machines on a 100 Mbps private Ethernet LAN, as shown in Figure 14. One machine serves as the TCP source node, with another as the TCP destination node, and the third as the network emulator.

The TCP source node was a 1.8 GHz Intel Pentium 4 machine with 512 MB of RAM, running the FreeBSD 4.11 operating system. We verified that the NewReno implementation in the FreeBSD kernel conformed to the TCP NewReno description in RFC 3782. In addition, we instrumented the FreeBSD kernel to collect statistics required for model validation such as the number of timeout (TO) events, the number of fast recovery (FR) events, the total transfer duration (in seconds), the total bytes successfully transferred (Bytes), and the fine-grained RTT. The TCP destination node was a 2.8 GHz Intel Xeon with 1 GB of RAM. This machine was running Linux 2.6.8 as the operating system.

We used `iperf`⁸ for generating TCP bulk data transfers. This software, freely available from NLANR, is used for measuring TCP and UDP performance. In our experiments, we ran `iperf` in the TCP-mode to generate traffic representing bulk data transfer.

We used the Internet Protocol and Traffic Network Emulator (IP-TNE) [38] to emulate a wide area network. IP-TNE is a high-performance internetwork emulation tool that uses a parallel discrete-event simulation kernel. In our experiments, all `iperf` traffic between the TCP source and TCP destination traverses the virtual (simulated) wide area network. IP-TNE transfers IP packets as needed between the real and the simulated network, and models packet transmissions in the emulated wide area network. IP-TNE was running on a 3.2 GHz Intel Xeon machine with 4 GB of RAM; the operating system on this machine was Red Hat Enterprise Linux Academic Server Edition 4.

B. Emulated Network

The experiments reported here use a simple dumbbell network topology. There is a single bottleneck link of capacity 10 Mbps between the TCP source node and the TCP sink node. The TCP source and destination nodes are each connected to the bottleneck link by a 100 Mbps access link. In the experiments, the round-trip propagation delay of the emulated network is 50 ms.

All routers in the emulated network use FIFO queueing, with DropTail queue management. We installed a Bernoulli packet drop module on the access link of the TCP destination node to drop packets at a predetermined rate. The buffer at the bottleneck router was sufficiently provisioned such that there were no congestion-induced packet losses. This setup is simple, but allows us to compare the emulation results with those from *ns-2* simulations.

C. Results

In our emulation experiments, we varied the imposed packet loss rate from 0.5% to 3%, in steps of 0.5%. Table III summarizes statistics obtained from the emulation experiments. Note

⁸<http://dast.nlanr.net/Projects/Iperf/>

TABLE III
SUMMARY OF EMULATION EXPERIMENTS

Loss Rate	TO	FR	RTT (ms)	Duration (sec.)	Bytes
0.50%	5	556	55.56	500.54	169,942,625
1.00%	21	765	57.31	502.33	116,768,593
1.50%	38	841	58.48	502.62	89,441,537
2.00%	68	864	59.06	501.92	72,544,825
2.50%	113	775	59.65	502.11	55,202,129
3.00%	129	777	60.23	502.92	47,554,586

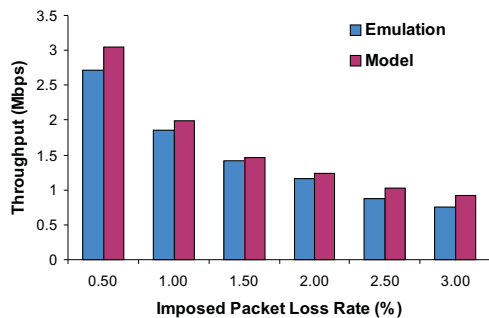


Fig. 15. Model Accuracy in WAN Emulation

that summing the number of FR and TO events represents the total number of loss events experienced by the TCP flow. The segment size (or *Segsize*) for all transfers is 1448 byte excluding TCP and IP headers. As in [29], we use the expression $\frac{FR+TO}{Bytes/Segsize}$ to estimate the loss event rate p . This computed loss event rate and the measured RTT are used as inputs to our “Full” TCP NewReno throughput model. In our computation of the model estimated throughputs, we used the approximation $q = p$.

In the absence of loss ($p=0\%$), the NewReno flow fully utilizes the 10 Mbps bottleneck link. The achieved throughput is 9.59 Mbps excluding TCP/IP header overhead, and 9.93 Mbps including TCP/IP overhead.

Figure 15 shows the (emulated) throughput attained by the TCP flow, along with the throughput predicted by our model. All these throughput calculations exclude the TCP/IP header overhead. At 1.5% imposed loss rate, the emulation throughput is 1.42 Mbps and the model prediction is 1.46 Mbps, correspondingly the prediction error is 3.0%. The maximum estimation error observed is 21% (at an imposed packet loss rate of 3%), and the average prediction error is 11%.

In general, our model predicts the TCP NewReno throughput successfully in the experiments considered.

VI. INTERNET EXPERIMENTS

As a final step for model validation, we conducted several experiments on the Internet. With help from selected colleagues around the globe, we measured the throughput achieved for 5 MB file transfers from our BSD Unix server site in Calgary to 6 different client locations: USA, Canada, UK, Australia, Bangladesh, and Japan. For space reasons, we only present results from the latter experiment, which had the worst-case prediction error observed.

TABLE IV
EXPERIMENTAL RESULTS FROM CALGARY TO JAPAN

Imposed PLR	TO	FR	Actual LER	RTT (ms)	Duration (sec)	Expt (Kbps)	Model (Kbps)
0.00%	7	27	0.98%	229	106.34	379	497 382*
0.50%	5	39	1.27%	245	120.12	335	394
1.00%	9	58	1.93%	237	134.84	299	297
1.50%	24	87	3.19%	253	195.73	206	202
2.50%	59	100	4.57%	256	277.23	145	147
2.00%	26	76	2.93%	300	302.13	133	173
3.00%	59	119	5.12%	260	290.15	139	141

To validate our model predictions at different loss rates, we added controlled levels of packet loss to our experiments using DummyNet [34]. We varied the imposed packet loss rate (PLR) from 0.5% to 3%, leaving bandwidth and delay unchanged. Actual losses always exceed the imposed PLR.

Table IV shows the results from the Japan experiment. The (Full) NewReno model predicts the observed throughputs reasonably well, with an average prediction error of 12%. These model predictions use the assumption $q = p$. The native network path (i.e., with zero imposed PLR) is lossy, experiencing a loss event rate (LER) of 0.98%, and a PLR of 6.21%. The prediction error for this case is high at 31%, because the average number of segment losses per loss event ($m = \frac{6.21}{0.98} = 6.4$) is relatively large, and the assumption $q = p$ is violated. Using $q = \frac{m-1}{W-1}$ in the model (denoted with ‘*’ in Table IV) reduces the prediction error to 0.94%.

VII. CONCLUSIONS

This paper presents an analytic model for the bulk data transfer performance of TCP NewReno. The model expresses steady-state throughput in terms of RTT and loss rate.

Our NewReno throughput model has three important features. First, we explicitly model the fast recovery algorithm of TCP NewReno, which is important since a NewReno flow may spend a significant amount of time in the fast recovery phase. Second, we also consider the possibility of incurring a timeout following an unsuccessful fast recovery phase. Third, our analytical model uses a flexible two-parameter loss model that captures both the loss event rate, as well as the burstiness of segment losses within a loss event, and thus is able to better capture the dynamics of TCP loss events on the Internet.

We validated our model with extensive *ns-2* simulation experiments. We also validated our model using a real TCP NewReno implementation. Our results show that the proposed model can predict steady-state TCP NewReno throughput for a wide range of network conditions, unlike existing Reno models. The results also illustrate the significant performance advantages of NewReno over Reno in many scenarios because of NewReno’s improved fast recovery algorithm.

Our *ns-2* simulation scripts are available from <http://www.cpsc.ucalgary.ca/~carey/software.html>. The authors thank Martin Arlitt, Derek Eager, Sally Floyd, Majid Ghaderi, and the ToN reviewers for constructive comments on earlier versions of this paper. Financial support for this work was provided by NSERC and iCORE.

REFERENCES

- [1] M. Allman. A Web Server's View of the Transport Layer. *ACM Computer Communications Review*, 30(5):10–20, October 2000.
- [2] E. Altman, K. Avrachenkov, and C. Barakat. A Stochastic Model of TCP/IP with Stationary Random Losses. In *Proc. of ACM SIGCOMM*, pages 231–242, Stockholm, Sweden, August 2000.
- [3] M. Arlitt and C. Williamson. Internet Web Servers: Workload Characterization and Performance Implications. *IEEE/ACM Transactions On Networking*, 5(5):631–645, October 1997.
- [4] D. Bansal and H. Balakrishnan. Binomial Congestion Control Algorithms. In *Proc. of IEEE INFOCOM*, pages 631–640, Anchorage, USA, April 2001.
- [5] L. Brakmo, S. O'Malley, and L. Peterson. TCP Vegas: New Techniques for Congestion Detection and Avoidance. In *Proc. of ACM SIGCOMM*, pages 24–35, New York, USA, August 1994.
- [6] N. Cardwell, S. Savage, and T. Anderson. Modeling TCP Latency. In *Proc. of IEEE INFOCOM*, pages 1742–1751, Tel-Aviv, March 2000.
- [7] K. Fall and S. Floyd. Simulation-Based Comparisons of Tahoe, Reno, and Sack TCP. *ACM Computer Communication Review*, 26(3):5–21, July 1996.
- [8] V. Firoiu and M. Borden. A Study of Active Queue Management for Congestion Control. In *Proc. of IEEE INFOCOM*, Tel-Aviv, Israel, March 2000.
- [9] S. Floyd. Connections with Multiple Congested Gateways in Packet-Switched Networks. *ACM Comp. Comm. Rev.*, 21(5):30–47, 1997.
- [10] S. Floyd and K. Fall. Promoting the Use of End-to-End Congestion Control in the Internet. *IEEE/ACM Transactions on Networking*, 7(4):458–472, 1999.
- [11] S. Floyd, R. Gummadi, and S. Shenker. Adaptive RED: An Algorithms for Increasing the Robustness of RED's Active Queue Management. Technical Report, August 2001.
- [12] S. Floyd, M. Handley, J. Padhye, and J. Widmer. Equation-Based Congestion Control for Unicast Applications. In *Proc. of ACM SIGCOMM*, pages 43–56, Stockholm, Sweden, August 2000.
- [13] S. Floyd, T. Henderson, and A. Gurtov. The NewReno Modification to TCP's Fast Recovery Algorithm. RFC 3782, April 2004.
- [14] S. Floyd and V. Jacobson. On Traffic Phase Effects in Packet-Switched Gateways. *Internetworking: Research and Experience*, 3(3):115–156, September 1992.
- [15] S. Floyd and E. Kohler. Internet Research Needs Better Models. In *Proc. of First Workshop on Hot Topics in Networking*, Princeton, USA, October 2002.
- [16] M. Goyal, R. Guerin, and R. Rajan. Predicting TCP Throughput from Non-Invasive Network Sampling. In *Proc. of IEEE INFOCOM*, Hiroshima, Japan, March 2002.
- [17] Q. He, C. Dovrolis, and M. Ammar. On the Predictability of Large Transfer TCP Throughput. In *Proc. of ACM SIGCOMM*, Philadelphia, USA, August 2005.
- [18] V. Jacobson. Congestion Avoidance and Control. In *Proc. of ACM SIGCOMM*, pages 314–329, Stanford, CA, USA, August 1988.
- [19] V. Jacobson. Berkeley TCP evolution from 4.3-Tahoe to 4.3 Reno. In *Proc. of the 18th IETF*, Vancouver, Canada, August 1990.
- [20] H. Jiang and C. Dovrolis. Passive Estimation of TCP Round-trip Times. *ACM Computer Communication Review*, 32(3):75–88, July 2002.
- [21] D. Kosti, A. Rodriguez, J. Albrecht, and A. Vahdat. Bullet: High Bandwidth Data Dissemination using an Overlay Mesh. In *Proc. of ACM SOSP*, Bolton Landing, USA, October 2003.
- [22] A. Kumar. Comparative Performance Analysis of Versions of TCP in a Local Network with a Lossy Link. *IEEE/ACM Transactions on Networking*, 6(4):485–498, August 1998.
- [23] T. Lakshman and U. Madhow. The Performance of TCP/IP for Networks with High Bandwidth-Delay Products and Random Loss. *IEEE/ACM Transactions on Networking*, 5(3):336–350, July 1997.
- [24] A. Mahanti, D. Eager, and M. Vernon. Improving Multirate Congestion Control Using a TCP Vegas Throughput Model. *Computer Networks*, 48(2):113–136, June 2005.
- [25] M. Mathis, J. Semke, J. Mahdavi, and T. Ott. The Macroscopic Behavior of the TCP Congestion Avoidance Algorithm. *ACM Computer Communication Review*, 27(3):67–82, July 1997.
- [26] A. Medina, M. Allman, and S. Floyd. Measuring the Evolution of Transport Protocols in the Internet. *Computer Communications Review*, 35(2):37–51, April 2005.
- [27] A. Misra and T. Ott. The Window Distribution for Idealized TCP Congestion Avoidance with Variable Packet Loss. In *Proc. of IEEE INFOCOM*, pages 1564–1572, New York, USA, March 1999.
- [28] V. Misra, W. Gong, and D. Towsley. Stochastic Differential Equation Modeling and Analysis of TCP-WindowSize Behavior. In *Proc. of IFIP Performance*, Istanbul, Turkey, October 1999.
- [29] J. Padhye, V. Firoiu, D. Towsley, and J. Kurose. Modeling TCP Throughput: A Simple Model and its Empirical Validation. In *Proc. of ACM SIGCOMM*, Vancouver, Canada, September 1998.
- [30] J. Padhye and S. Floyd. On Inferring TCP Behavior. In *Proc. of ACM SIGCOMM*, pages 287–298, San Deigo, USA, August 2001.
- [31] N. Parvez, A. Mahanti, and C. Williamson. TCP NewReno: Slow-but-Steady or Impatient? In *Proceedings of IEEE ICC 2006*, Istanbul, Turkey, June 2006.
- [32] V. Paxson. Empirically Derived Analytic Models of Wide-Area TCP Connections. *IEEE/ACM Trans. on Networking*, 2(4):316–336, 1994.
- [33] J. Postel. Transmission Control Protocol. RFC 793, September 1980.
- [34] L. Rizzo. Dummynet and Forward Error Correction. In *Proc. of Freenix*, New Orleans, USA, June 1998.
- [35] C. Samios and M. Vernon. Modeling the Throughput of TCP Vegas. In *Proc. of ACM SIGMETRICS*, San Diego, USA, June 2003.
- [36] B. Sikdar, S. Kalyanaraman, and K. Vastola. An Integrated Model for the Latency and Steady-State Throughput of TCP Connections. *Performance Evaluation*, 46(2-3):139–154, September 2001.
- [37] B. Sikdar, S. Kalyanaraman, and K. Vastola. Analytic Models for the Latency and Steady-State Throughput of TCP Tahoe, Reno and SACK. *IEEE/ACM Transactions on Networking*, 11(6):959–971, December 2003.
- [38] R. Simmonds, R. Bradford, and B. Unger. Applying Parallel Discrete Event Simulation to Network Emulation. In *Proc. ACM Parallel and Distributed Simulation*, pages 15–22, Bologna, Italy, May 2000.
- [39] W. Stevens. *TCP/IP Illustrated Vol. 1: The Protocols*. Addison-Wesley, Boston, USA, 1994.
- [40] W. Stevens and G. Wright. *TCP/IP Illustrated Vol. 2: The Implementation*. Addison-Wesley, Boston, USA, 1995.
- [41] M. Yajnik, S. Moon, J. Kurose, and D. Towsley. Measurement and Modeling of the Temporal Dependence in Packet Loss. In *Proc. of IEEE INFOCOM*, pages 345–352, New York, NY, March 1999.

Nadim Parvez is a Ph.D. candidate in the Department of Computer Science at the University of Calgary. He holds a B.E. in Computer Science and Engineering from the Bangladesh University of Engineering Technology and a M.Sc. in Electrical and Computer Engineering from the University of Manitoba. His research interests include Internet protocols, TCP modeling, peer-to-peer systems, and media streaming systems.



Anirban Mahanti is a Senior Researcher at NICTA. He holds a B.E. in Computer Science and Engineering from the Birla Institute of Technology (at Mesra), India, and a M.Sc. and a Ph.D. in Computer Science from the University of Saskatchewan. His research interests include network measurement, TCP/IP protocols, performance evaluation, and distributed systems.



Carey Williamson is a Professor in the Department of Computer Science at the University of Calgary, where he holds an iCORE Chair in *Broadband Wireless Networks, Protocols, Applications, and Performance*. He has a B.Sc.(Honours) in Computer Science from the University of Saskatchewan, and a Ph.D. in Computer Science from Stanford University. His research interests include Internet protocols, wireless networks, network traffic measurement, network simulation, and Web performance.

